

This discussion paper is/has been under review for the journal Atmospheric Chemistry and Physics (ACP). Please refer to the corresponding final paper in ACP if available.

**Impact of aerosol
composition**

Q. Zhang et al.

Impact of aerosol composition on cloud condensation nuclei activity

Q. Zhang¹, J. Meng¹, J. Quan^{1,2}, Y. Gao¹, D. Zhao¹, P. Chen¹, and H. He¹

¹Beijing Weather Modification Office, Beijing, China

²Institute of Urban Meteorology, CMA, Beijing, China

Received: 24 October 2011 – Accepted: 29 November 2011 – Published: 17 January 2012

Correspondence to: J. Quan (quanjn1975@gmail.com)

Published by Copernicus Publications on behalf of the European Geosciences Union.

Title Page

Abstract

Introduction

Conclusions

References

Tables

Figures

◀

▶

◀

▶

Back

Close

Full Screen / Esc

Printer-friendly Version

Interactive Discussion



Abstract

The impact of aerosol composition on cloud condensation nuclei (CCN) activity was analyzed in this study based on field experiments carried out at downtown Tianjin, China, in September 2010. In the experiments, the CCN measurements were performed at supersaturation (SS) of 0.1 %, 0.2 % and 0.4 % using a thermal-gradient diffusion chamber (DMT CCNC), whereas the aerosol size distribution and composition were simultaneously measured with a TSI SMPS and an Aerodyne Aerosol Mass Spectrometer (AMS), respectively. The results show that the influence of aerosol composition on CCN activity is notable under low SS (0.1 %), and their influence decreased with increasing SS. For example, under SS of 0.1 %, the CCN activity increases from 4.5 ± 2.6 % to 12.8 ± 6.1 % when organics fraction decrease from 30–40 % to 10–20 %. The rate of increase reaches up to 184 %. While under SS of 0.4 %, the CCN activity increases only from 35.7 ± 19.0 % to 46.5 ± 12.3 %, correspondingly. The calculated N_{CCN} based on the size-resolved activation ratio and aerosol number size distribution correlates well with observed N_{CCN} at high SS (0.4 %), but this correlation decreases with the falling of SS. The slopes of linear fitted lines between calculated and observed N_{CCN} are 0.708, 0.947, and 0.995 at SS of 0.1 %, 0.2 % and 0.4 %, respectively. Moreover, the standard deviation (SD) of calculated N_{CCN} increases with the decreasing of SS. A case study of CCN closure analyses indicates that the calculated error of N_{CCN} can reach up to 34 % at SS of 0.1 % if aerosol composition is not included, and the calculated error decreases with the raising of SS. It decreases to 9 % at SS of 0.2 %, and further decreases to 4 % at SS of 0.4 %.

1 Introduction

Part of aerosol particles can act as cloud condensation nuclei (CCN), which will affect cloud formation (Ramanathan et al., 2001; Andreae et al., 2004), including cloud droplet number concentration and their size (Jin and Shepherd, 2008; Rosenfeld et al.,

ACPD

12, 1493–1516, 2012

Impact of aerosol composition

Q. Zhang et al.

Title Page

Abstract

Introduction

Conclusions

References

Tables

Figures

◀

▶

◀

▶

Back

Close

Full Screen / Esc

Printer-friendly Version

Interactive Discussion



2008; Zhang et al., 2011). The complexities of aerosol particles make it rather difficult to estimate their CCN activity (Cruz and Pandis, 1998; Hegg et al., 2001; Prenni et al., 2001; Brooks et al., 2003; Kumar et al., 2003; Raymond and Pandis, 2003; Broekhuizen et al., 2004; Marcolli et al., 2004; Henning et al., 2005), which means that the impact of aerosol on cloud and the cloud feedbacks are currently considered as the largest uncertainties in climate system (IPCC, 2007).

The ability of an aerosol particle to become a droplet is primarily a function of its size and chemical composition (Seinfeld and Pandis, 2006). Köhler theory describes the competing effects involved in cloud droplet activation. Two competing effects determine the equilibrium vapor pressure of water over an aqueous solution droplet: the solution effect (Raoult's law), which tends to decrease the equilibrium vapor pressure on the droplet; and the curvature (Kelvin's law) effect, which tends to increase the equilibrium vapor pressure on the droplet. Compared with organics, the solution of inorganic salts are much higher, which makes the inorganic salts easier to be activated. For example, the critical supersaturation (S_c) needed to activate particles of ammonium sulfate and adipic acid of size 100 nm are 0.15% and 0.27%, respectively (Hings et al., 2008). Moreover, the presence of slight soluble aerosol particles or soluble gases will further decrease the S_c (Kulmala et al., 1997). The work of Kulmala et al. (1997) reveals that stable cloud droplets of size 1–10 μm could exist in air with a relative humidity of less than 100%. Therefore, the SS should be considered during an experiment that studies the effect of aerosol composition on CCN activation. If the SS is set too high, the component properties of aerosol particles might be masked.

In this study, a field experiment was conducted in a heavy pollution area located in the North China Plain (NCP). During the experiment, the aerosol number size distribution, composition (sulfate, nitrate, ammonium, chlorite, organics), and the size-resolved activation ratio under different SS (0.1–0.4%) were measured. A large variability of the ratio of organics to inorganic salts was observed during the field experiment, providing a good opportunity to study the effect of aerosol composition on CCN activity under different SS.

Impact of aerosol composition

Q. Zhang et al.

[Title Page](#)[Abstract](#)[Introduction](#)[Conclusions](#)[References](#)[Tables](#)[Figures](#)[◀](#)[▶](#)[◀](#)[▶](#)[Back](#)[Close](#)[Full Screen / Esc](#)[Printer-friendly Version](#)[Interactive Discussion](#)

2 Experimental methods

2.1 Aerosol sampling site

The sampling site is situated in the northwest of the urban area of Tianjin, and the measurements were conducted continuously from 1 September to 26 September 2010. The monitoring instruments were deployed on a monitor station with no high buildings around. A main road about 20 m away to the north passes by the monitor station, and no significant pollution sources exist near the sampling site.

During the campaign, sampling of aerosol was conducted from the top of the sampling room via a PM_{2.5} cyclone inlet which can remove coarse particles more than 2.5 μm. To minimize sampling losses, a stainless steel pipe, approximately 1/4 inch in diameter, was used to introduce air stream into the room. During the campaign, the air-conditioned room temperature was ~21° and the sampling air relative humidity (RH) was maintaining below 30 % after passing through two diffusion dryers.

2.2 Instrument setup

Polydisperse dry aerosol was charge-neutralized using a Kr-85 neutralizer (TSI 3077A) and introduced into a differential mobility analyzer (DMA, TSI 3081L) for classification by electrical mobility. The classified aerosol was then split into a condensation particle counter (CPC, TSI 3776) to measure the particle size distribution and the total aerosol concentration (condensation nuclei, CN), and into a DMT double-column continuous-flow CCN counter (CCN-200) (Roberts and Nenes, 2005; Lance et al., 2006) to obtain the CCN activation properties. The particle size distribution was measured every 5 min, with an up-scan time of 280 s. The DMA was operated with 0.8 l min⁻¹ sample air flow rate, which was split into two parts with 0.5 l min⁻¹ for CCN counter and 0.3 l min⁻¹ for CPC, and a closed-loop sheath air flow rate of 8 l min⁻¹. The sheath flow rate was continuously regulated to a constant volumetric flow, using a mass flow controller with a continuous pressure- and temperature-compensated mass flow set point. All flow rates

Title Page

Abstract

Introduction

Conclusions

References

Tables

Figures

◀

▶

◀

▶

Back

Close

Full Screen / Esc

Printer-friendly Version

Interactive Discussion



were regularly checked and sizing accuracy was checked by employing Polystyrene latex (PSL) spheres with different diameters.

The CCN-200 has two columns to measure different samples at different supersaturations (SS) at the same time. In the field experiment, column A directly measured the dry polydisperse aerosol sample to obtain the bulk CCN concentration, while column B was connected to the exit of DMA to measure the size-resolved particles activation properties. The CCN-200 was operated at a total flow rate of 1 l min^{-1} with a sheath-to-aerosol flow ratio of 10. Both columns operated at the same SS at the same time. One measurement cycle included measurements at 5 different SS (0.07 %, 0.10 %, 0.20 %, 0.40 % and 0.80 %) of 20 min for 0.07 % and 10 min for each of the rest. Therefore, the N_{CCN} for five SS were available every hour. Here, 10 min per SS can ensure at least two replicates per SS, as CCN temperature transients during SS changes may produce unreliable spectra if they occur during a voltage up-scan (Moore et al., 2010). Whenever the temperature gradient is changed, up to 2 min are required for the instrument profiles to stabilize.

The Dual CCN counter was calibrated regularly with size selected (by DMA) ammonium sulfate particles (Rose et al., 2008; Deng et al., 2011) before and after the campaign. The critical dry diameters (50 % of the particles activated) determined from the activation curves of ammonium sulfate under different temperature gradients (TG) were converted to SS utilizing the Köhler equation where several Köhler theory parameters employed (Cooper and Dooley, 1994; Seinfeld and Pandis, 2006; Young and Warren, 1992; Low, 1969). TG and SS were linearly fitted. The SS of CCN was calculated from the TG-SS linearly fitted function.

The aerosol chemical composition of the non-refractory submicron particles was measured by an Aerodyne Compact Time-of-Flight Aerosol Mass Spectrometer (C-ToF-AMS). The detail description of the C-ToF-AMS and its operation have been presented in many previous publications and reviewed by Drewnick et al. (2005). In short, ambient aerosol is focused through an aerodynamic lens assembly into a narrow particle beam for sizes between 50 nm and 600 nm efficiently (Zhang et al., 2002, 2004).

Impact of aerosol composition

Q. Zhang et al.

[Title Page](#)[Abstract](#)[Introduction](#)[Conclusions](#)[References](#)[Tables](#)[Figures](#)[◀](#)[▶](#)[◀](#)[▶](#)[Back](#)[Close](#)[Full Screen / Esc](#)[Printer-friendly Version](#)[Interactive Discussion](#)

Impact of aerosol composition

Q. Zhang et al.

[Title Page](#)[Abstract](#)[Introduction](#)[Conclusions](#)[References](#)[Tables](#)[Figures](#)[◀](#)[▶](#)[◀](#)[▶](#)[Back](#)[Close](#)[Full Screen / Esc](#)[Printer-friendly Version](#)[Interactive Discussion](#)

Smaller and larger particles are also collected, but with lower efficiency. Particle size information was obtained by measuring particle velocity with a mechanical chopper wheel: The particles impact on an inverted conical tungsten vapour, where the non-refractory components are flash vapour. Then the resulting gas is ionised by electron ionization at 70 eV. The ions are subsequently extracted orthogonally and sampled by the C-ToF-AMS (Tofwerk AG, Thun, Switzerland) for mass analysis. The instrument provides 2 min averaged quantitative mass loading information on non-refractory components using a well characterised series of calibrations and error estimations (Jimenez et al., 2003; Allan et al., 2003, 2004), as well as species resolved size distributions. The C-ToF-AMS calibration, e.g. inlet flow, ionization efficiency (IE) and particle sizing, was performed at the beginning, the middle and the end of the campaign as the standard protocols recommend (Jayne et al., 2000; Jimenez et al., 2003; Drewnick et al., 2005).

2.3 Data processing

The CN and CCN time series distribution was obtained by using the TSI Aerosol Instrument Manager (AIM) software (Wang and Flagan, 1989) and CCN acquiring software, respectively. AIM provided the raw CN counts reported by the CPC every 0.1 s during each scan cycle and CCN acquiring software recorded data every second. Here data collected during the voltage upscan was employed to inversion. The detail description of the application of Scanning Mobility CCN Analysis (SMCA) and the CCN activation ratio calculation are introduced by Moore et al. (2010). Firstly, the time series distribution of CN and CCN is aligned by matching the minimum in counts that occurs during the transition between upscan and downscan. Then the CN and CCN time series is converted to size space using the size-scan time relationship provided by the AIM software, the inverted size-resolved aerosol number distribution is obtained. Finally, a multiple charged correction is applied for the CCN activation ratio calculation due to the presence of multiply charged particles, which will result higher measured activation ratio especially for these smaller particle sizes.

The C-ToF-AMS usually has two different operational modes: (i) the MS (Mass Spectrum) mode which is used to collect averaged mass spectra of the non-refractory aerosol and can provide mass concentrations for several species such as sulfate, nitrate, ammonium, chloride and total non-refractory organics; and (ii) the P-ToF (Particle Time-of-Flight) mode which is used to collect averaged size distribution data for all non-refractory aerosol and can calculate size distributions for each species independently. Therefore, the C-ToF-AMS can provide redundant as well as complementary information of chemistry and size distribution for the non-refractory aerosol. Details of the inversions are presented by Drewnick et al. (2005) and DeCarlo et al. (2006).

3 Results and discussion

3.1 Sampling data

Figure 1 shows the sampling data at downtown Tianjin during 1–7 and 15–23 September 2010. The hourly-averaged mass concentration of aerosol particles observed by AMS range from 4 to 251 $\mu\text{g cm}^{-3}$, with averaged mass concentration of $66 \pm 50 \mu\text{g cm}^{-3}$. Large variation of aerosol composition was observed during this experiment. Hourly-averaged organics fraction range from 1.1 % to 63.8 %, with 82 % data ranges from 10–60 %. The averaged mass component of aerosols during the experiment are: organics, 23.8 %; sulfate (SO₄), 21.8 %; nitrite (NO₃), 24.6 %; ammonia (NH₄), 20.6 %; chlorine (Cl), 9.2 %. The number concentration of aerosol particles with size of 14.1–736.5 nm observed by SMPS range from 2416 to 32 396 cm^{-3} with an averaged value of $13117 \pm 4797 \text{ cm}^{-3}$. The averaged number concentrations of CCN under SS of 0.1 %, 0.2 %, 0.4 % are $1489 \pm 982 \text{ cm}^{-3}$, $4121 \pm 2725 \text{ cm}^{-3}$, $6640 \pm 6791 \text{ cm}^{-3}$, respectively. Large variation of CCN/CN was also observed during this experiment. The CCN/CN under SS of 0.1 %, 0.2 %, 0.4 % range from 0.6 %-32.6 %, 5.2 %-55.6 %, 8.8 %-75.7 %, respectively.

[Title Page](#)[Abstract](#)[Introduction](#)[Conclusions](#)[References](#)[Tables](#)[Figures](#)[◀](#)[▶](#)[◀](#)[▶](#)[Back](#)[Close](#)[Full Screen / Esc](#)[Printer-friendly Version](#)[Interactive Discussion](#)

3.2 Effect of aerosol composition on CCN activity

CCN is the aerosol particles that can grow into cloud droplets (activate) under atmospheric SS. The SS needed to activate the particles is called critical supersaturation (S_c). Based on Köhler theory, for particles of constant size, the S_c depends on its solution, which is a function of its composition (Dusek et al., 2006), including the number of potential solute molecules and the solution it contains. For example, the S_c needed to activate the particles of ammonium sulfate, adipic acid with size of 100 nm is 0.15 % and 0.27 %, respectively (Hings et al., 2008). With the increasing of SS, the CCN/CN will increase correspondingly. Therefore, the SS should also be considered in studying the CCN activation of environment aerosols. If the SS is set too high in the experiment, the properties of aerosol particles might be masked. In the atmosphere, aerosol particles are most likely to be mixtures of organic and inorganic components. Based on Köhler theory, the S_c needed for inorganic salts to activate to CCN is lower than organics for the same size of particles due to the high solution of inorganic salts, which makes particles with more inorganic salts easier to be activated under the same condition. In this study, the organics fraction measured by AMS was used to analyze the effect of aerosol composition on CCN activity.

Figures 2 and 3 shows the relation of CCN/CN, and the diameter of particles at CCN/CN = 0.5 (D_{p50}) with organics fraction under the three SS, respectively. Under a certain SS, the CCN/CN decreased with the raising of organics fraction. Moreover, the decreasing trend is more effective under lower SS. For example, under SS of 0.1 %, the CCN/CN increased from 4.5 ± 2.6 % to 12.8 ± 6.1 % when organics fraction decreased from 30–40 % to 10–20 %. The rate of increase reached up to 184 %. While under SS of 0.4 %, the CCN activity increased only from 35.7 ± 19.0 % to 46.5 ± 12.3 %, correspondingly, and the rate of increasing decreased to 30.1 %. In Fig. 2, the size of particles were not included. To analyze the influence of particles size on CCN activity under different aerosol composition, we compared the relation of D_{p50} with organics fraction. The D_{p50} increased correspondingly with the raising of organics fraction, indicating

Impact of aerosol composition

Q. Zhang et al.

[Title Page](#)[Abstract](#)[Introduction](#)[Conclusions](#)[References](#)[Tables](#)[Figures](#)[◀](#)[▶](#)[◀](#)[▶](#)[Back](#)[Close](#)[Full Screen / Esc](#)[Printer-friendly Version](#)[Interactive Discussion](#)

that less particles will be converted to CCN. For example, under SS of 0.1 %, the D_{p50} increased from 152.3 ± 7.1 nm to 163.4 ± 11.1 nm when organics fraction raised from 10–20 % to 30–40 %. The extent of increase was 11.1 nm. While under SS of 0.2 %, the extent of increase declined to 6.5 nm, and further declined to 4.2 nm at SS of 0.4 %.

3.3 Size-resolved activation ratio

Based on the observations and methods introduced at Sect. 2, we first calculated the CCN activity (Fig. 4) and their standard deviation (SD) (Fig. 5) under the three SS with-out consideration of aerosol composition. The standard deviation (SD) of the spectrum regarding CCN activity is defined as follow:

$$SD = \left(\sum (r - \bar{r})^2 / N \right)^{1/2} \quad (1)$$

where r is the ratio of CCN to CN, \bar{r} is averaged data, and N is sample number.

Figure 4 shows that the CCN activity is highly sensitive to SS for particles with size of 50–200 nm, which is the dominant fraction of aerosol particles. For example, for particles with size of 100 nm, the CCN/CN is near to 0 at SS of 0.1 %, and increases to 0.75 at SS of 0.2 %, then further increases to near 1.0 at SS of 0.4 %. The SD in our observation fluctuated with SS and particle size. It decreased with the increasing of particle size for a certain SS, while the SD decreases with the increasing of SS for all particles (Fig. 5). For example, under constant SS of 0.1 %, the SD was 4.2, 0.8, and 0.09 at size of 100 nm, 150 nm and 200 nm, respectively. While for particles with size of 100 nm, the SD was 0.04, 0.2, and 4.2 at SS of 0.4 %, 0.2 % and 0.1 %, respectively. The high SD for small particles (50–200 nm) at low SS (0.1 %) might be caused by the variation of the aerosol composition since their effect on CCN activation was observed (Fig. 5), especially at low SS.

The CCN concentration ($N_{CCN, Cal}$) can be calculated using the following equation:

$$N_{CCN, Cal} = \int A(\log D_p) n(\log D_p) d \log D_p \quad (2)$$

Title Page

Abstract

Introduction

Conclusions

References

Tables

Figures

◀

▶

◀

▶

Back

Close

Full Screen / Esc

Printer-friendly Version

Interactive Discussion



where $A(\log D_p)$ is the size resolved activation ratio, and $n(\log D_p)$ is the function of the aerosol number size distribution.

The calculated N_{CCN} based on Eq. (2), the size-resolved activation ratios (Fig. 4) and observed aerosol number size distribution is highly consistent with the measured N_{CCN} (Fig. 6) at high SS ($R^2 = 0.9925$ at SS of 0.4 %) and the consistent decreased with decreasing of SS ($R^2 = 0.9480$ at SS of 0.1 %). The linear fitted lines have slopes lower than 1 for each SS. The slopes are 0.708, 0.947, and 0.995 at SS of 0.1 %, 0.2 % and 0.4 %, respectively.

The above analysis indicates that the effect of aerosol composition on CCN cannot be ignored in estimating the CCN concentration, especially at low SS which is present at natural environment. For example, the typical SS for stratiform clouds and fog are 0.05 % and 0.1 %, respectively (Seinfeld and Pandis, 2006). To estimate quantitatively the contribution of aerosol composition on CCN calculated error, two cases of CCN closure study were analyzed with organics fraction of 24 % and 55 %, as described in the next section.

3.4 Contribution of aerosol composition on CCN calculated error

The selected two cases are for 4 and 20 September 2010. Figure 7 shows the daily averaged composition of the two days with sizes ranging from 50 to 200 nm. On 4 Sep, inorganic is the dominated component, which takes up 60–80 % in mass concentration, while on 20 Sep, organic is the dominated component, which takes up 40–70 % in mass concentration. The size-resolved CCN activation of aerosol particles under different SS calculation using methods introduced in Sect. 3.3 for observations on 4 and 20 Sep are shown in Fig. 8. There are significant differences of CCN/CN for particle sizes of 100–200 nm between the two cases under low SS (0.1 %). Moreover, the differences go down with the increasing of SS. For example, for particles with size of 150 nm, the CCN/CN is only 0.03 on 20 Sep, while it increases to 0.6 on 4 Sep. To estimate roughly the influence of aerosol composition on CCN activation, we calculate the N_{CCN} based

Impact of aerosol composition

Q. Zhang et al.

[Title Page](#)[Abstract](#)[Introduction](#)[Conclusions](#)[References](#)[Tables](#)[Figures](#)[◀](#)[▶](#)[◀](#)[▶](#)[Back](#)[Close](#)[Full Screen / Esc](#)[Printer-friendly Version](#)[Interactive Discussion](#)

on the CCN activation ratio extracted from the two cases at the same time and compare their differences. The calculated error is 31 % at SS of 0.1 %, decreases to 9 % at SS of 0.2 %, and further decreases to 4 % at SS of 0.4 %. Above results indicate that the influence of aerosol composition on CCN activation cannot be neglected under low SS since their compositions display great regional and temporal differences (Zhang et al., 2009).

4 Summaries

We conducted a field experiment carried out at downtown Tianjin during September 2010 to analyze the effect of aerosol composition on CCN activity. During this experiment, CCN concentration under SS of 0.1 %, 0.2 % and 0.4 %, together with the aerosol size distribution and composition, were simultaneously measured. Using the size and composition information, detailed CCN closure analyses under different SS were performed. The results are summarized as the follows:

1. The effect of aerosol composition on CCN activity is significant at low SS, and this effect decreases with the raising of SS. In this study, the fraction of organic component was used to represent character of aerosol composition in analyzing their influence on CCN activity. The observations indicate that the CCN activity decreases, and the D_{p50} increases with the raising of organic fraction. Moreover, the decreasing trend is more effective under lower SS. For example, under SS of 0.1 % the CCN activity increases from 4.5 ± 2.6 % to 12.8 ± 6.1 % when organic fraction decreases from 30–40 % to 10–20 %; the rate of increases reaches up to 184 %. While under SS of 0.4 %, the CCN activity increases only from 35.7 ± 19.0 % to 46.5 ± 12.3 %, correspondingly.
2. Regardless of aerosol composition, the calculated N_{CCN} based on the aerosol number size distribution and the size-resolved activation ratios are consistent with observed N_{CCN} at high SS (0.4 %), but this correlation decreases with the falling

Impact of aerosol composition

Q. Zhang et al.

Title Page

Abstract

Introduction

Conclusions

References

Tables

Figures

◀

▶

◀

▶

Back

Close

Full Screen / Esc

Printer-friendly Version

Interactive Discussion



Impact of aerosol composition

Q. Zhang et al.

Title Page

Abstract

Introduction

Conclusions

References

Tables

Figures

◀

▶

◀

▶

Back

Close

Full Screen / Esc

Printer-friendly Version

Interactive Discussion



of SS. Moreover, the standard deviation (SD) of calculated N_{CCN} increases with the decreasing of SS. The slopes of linear fitted lines between calculated N_{CCN} and observed N_{CCN} are 0.708, 0.947, and 0.995 at SS of 0.1 %, 0.2 % and 0.4 %, respectively.

3. The contribution of aerosol composition on CCN activity was estimated quantitatively based on CCN closure study of two cases with organic fraction of 24 % and 55 %. The calculated error is estimated on the difference of the calculated N_{CCN} based on size-resolved activation ratios extracted from the two cases. The result indicates that the calculated error of N_{CCN} could reach up to 34 % at SS of 0.1 % and that the calculated error decreases with the raising of SS. It decreases to 9 % at SS of 0.2 %, and further decreases to 4 % at SS of 0.4 %.

Acknowledgements. This research is partially supported by National Natural Science Foundation of China (NSFC) under Grant No. 40905060 and No. 41175007; The National Basic Research Program of China (2011CB403401); The project of scientific and technological new star of Beijing under Grant No. 2010B029; China Meteorological Administration (CMA) under Grant No GYHY200806001-4.

References

- Allan, J. D., Jimenez, J. L., Coe, H., Bower, K. N., Williams, P. I., and Worsnop, D. R.: Quantitative sampling using an aerodyne aerosol mass spectrometer, Part 1: Techniques of data interpretation and error analysis, *J. Geophys. Res. Atmos.*, 108, 4090, doi:10.1029/2002JD002358, 2003.
- Allan, J. D., Coe, H., Bower, K. N., Alfarra, M. R., Delia, A. E., Jimenez, J. L., Middlebrook, A. M., Drewnick, F., Onasch, T. B., Canagaratna, M. R., Jayne, J. T., and Worsnop, D. R.: Technical note: extraction of chemically resolved mass spectra from aerodyne aerosol mass spectrometer data, *J. Aerosol Sci.*, 35, 909–922, 2004.
- Andreae, M. O., Rosenfeld, D., Artaxo, P., Costa, A. A., Frank, G. P., Longo, K. M., and Silva-Dias, M. A. F.: Smoking rain clouds over the Amazon, *Science* 303, 1337–1342, 2004.

Impact of aerosol composition

Q. Zhang et al.

Title Page

Abstract

Introduction

Conclusions

References

Tables

Figures

◀

▶

◀

▶

Back

Close

Full Screen / Esc

Printer-friendly Version

Interactive Discussion



- Broekhuizen, K., Kumar, P. P., and Abbatt, J. P. D.: Partially soluble organics as cloud condensation nuclei: Role of trace soluble and surface active species, *Geophys. Res. Lett.*, **31**, L01107, doi:10.1029/2003GL018203, 2004.
- Brooks, S. D., Garland, R. M., Wise, M. E., Prenni, A. J., Cushing, M., Hewitt, E., and Tolbert, M. A.: Phase changes in internally mixed maleic acid/ammonium sulfate aerosols, *J. Geophys. Res.*, **108**, 4487, doi:10.1029/2002JD003204, 2003.
- Cooper, J. R. and Dooley, R. B.: IAPWS release on surface tension of ordinary water substance, available at: <http://www.iapws.org/relguide/surf.pdf>, 1994.
- Cruz, C. N. and Pandis, S. N.: The effect of organic coatings on the cloud condensation nuclei activation of inorganic atmospheric aerosol, *J. Geophys. Res.*, **103**, 13111–13123, 1998.
- DeCarlo, P. F., Kimmel, J. R., Trimborn, A., Northway, M. J., Jayne, J. T., Aiken, A. C., Gonin, M., Fuhrer, K., Horvath, T., Docherty, K. S., Worsnop, D. R., and Jimenez, J. L.: Field-deployable, high-resolution, time-of-flight aerosol mass spectrometer, *Anal. Chem.*, **78**, 8281–8289, 2006.
- Deng, Z. Z., Zhao, C. S., Ma, N., Liu, P. F., Ran, L., Xu, W. Y., Chen, J., Liang, Z., Liang, S., Huang, M. Y., Ma, X. C., Zhang, Q., Quan, J. N., Yan, P., Henning, S., Mildenberger, K., Sommerhage, E., Schäfer, M., Stratmann, F., and Wiedensohler, A.: Size-resolved and bulk activation properties of aerosols in the North China Plain, *Atmos. Chem. Phys.*, **11**, 3835–3846, doi:10.5194/acp-11-3835-2011, 2011.
- Drewnick, F., Hings, S. S., DeCarlo, P., Jayne, J. T., Gonin, M., Fuhrer, K., Weimer, S., Jimenez, J. L., Demerjian, K. L., Borrmann, S., Worsnop, D. R.: A new Time-of-Flight Aerosol Mass Spectrometer (TOF-AMS)– instrument description and first field deployment, *Aerosol Sci. Technol.*, **39**, 637–658, 2005.
- Dusek, U., Frank, G. P., Hildebrandt, Curtius, J., Schneider, J., Walter, S., Chand, D., Drewnick, F., Hings, S., Jung, D., Borrmann, S., and Andreae, M. O.: Size matters more than chemistry for cloud nucleating ability of aerosol particles, *Science*, **312**, 1375–1378, 2006.
- Hegg, D. A., Gao, S., Hoppel, W., Frick, G., Caffrey, P., Leaitch, W. R., Shantz, N., Ambrusko, J., and Albrechtski, T.: Laboratory studies of the efficiency of selected organic aerosols as CCN, *Atmos. Res.*, **58**, 155–166, 2001.
- Henning, S., Rosenrn, T., D’Anna, B., Gola, A. A., Svenningsson, B., and Bilde, M.: Cloud droplet activation and surface tension of mixtures of slightly soluble organics and inorganic salt, *Atmos. Chem. Phys.*, **5**, 575–582, doi:10.5194/acp-5-575-2005, 2005.
- Hings, S. S., Wrobel, W. C., Cross, E. S., Worsnop, D. R., Davidovits, P., and Onasch, T. B.:

Impact of aerosol composition

Q. Zhang et al.

Title Page

Abstract

Introduction

Conclusions

References

Tables

Figures

◀

▶

◀

▶

Back

Close

Full Screen / Esc

Printer-friendly Version

Interactive Discussion



CCN activation experiments with adipic acid: effect of particle phase and adipic acid coatings on soluble and insoluble particles, *Atmos. Chem. Phys.*, 8, 3735–3748, doi:10.5194/acp-8-3735-2008, 2008.

IPCC: *Climate Change 2007: The Physical Science Basis*, Cambridge University Press, Cambridge, United Kingdom and New York, NY, USA, 996 pp., 2007.

Jayne, J. T., Leard, D. C., Zhang, X., Davidovits, P., Smith, K. A., Kolb, C. E., and Worsnop, D. R.: Development of an Aerosol Mass Spectrometer for Size and Composition, Analysis of Submicron Particles, *Aerosol Sci. Technol.*, 33, 49–70, 2000.

Jin, M. and Shepherd, J. M.: Aerosol relationships to warm season clouds and rainfall at monthly scales over east China: Urban land versus ocean, *J. Geophys. Res.*, 113, D24S90, doi:10.1029/2008JD010276, 2008.

Jimenez, J. L., Jayne, J. T., Shi, Q., Kolb, C. E., Worsnop, D. R., Yourshaw, I., Seinfeld, J. H., Flagan, R. C., Zhang, X., Smith, K. A., Morris, J. W., and Davidovits, P.: Ambient aerosol sampling using the Aerodyne aerosol mass spectrometer, *J. Geophys. Res.*, 108, 8425–8437, 2003.

Kulmala, M., Laaksonen, A., Charlson, R. J., and Korhonen, P.: Clouds without supersaturation, *Nature*, 388, 336–337, 1997.

Pradeep Kumar, P., Broekhuizen, K., and Abbatt, J. P. D.: Organic acids as cloud condensation nuclei: Laboratory studies of highly soluble and insoluble species, *Atmos. Chem. Phys.*, 3, 509–520, doi:10.5194/acp-3-509-2003, 2003.

Lance, S., Medina, J., Smith, J. N., and Nenes, A.: Mapping the operation of the dmt continuous flow CCN counter, *Aerosol Sci. Technol.*, 40, 242–254, 2006.

Low, R. D. H.: A generalized equation for the solution effect in droplet 1 growth, *J. Atmos. Sci.*, 26, 608–611, 1969.

Marcolli, C., Luo, B. P., and Peter, T.: Mixing of the organic aerosol fractions: Liquids as the thermodynamically stable phases, *J. Phys. Chem.*, 108, 2216–2224, 2004.

Moore, R. H., Nenes, A., and Medina, J.: Scanning mobility CCN analysis – a method for fast measurements of size-resolved CCN distributions and activation kinetics, *Aerosol Sci. Tech.*, 44, 861–871, 2010.

Prenni, A. J., DeMott, P. J., Kreidenweis, S. M., Sherman, D. E., Russell, L. M., and Ming, Y.: The effects of low molecular weight dicarboxylic acids on cloud formation, *J. Phys. Chem.*, 105, 11240–11248, 2001.

Ramanathan, V., Crutzen, P. J., Lelieveld, J., Mitra, A. P., Althausen, D., Anderson, J., Andreae,

Impact of aerosol composition

Q. Zhang et al.

[Title Page](#)[Abstract](#)[Introduction](#)[Conclusions](#)[References](#)[Tables](#)[Figures](#)[◀](#)[▶](#)[◀](#)[▶](#)[Back](#)[Close](#)[Full Screen / Esc](#)[Printer-friendly Version](#)[Interactive Discussion](#)

M. O., Cantrell, W., Cass, G. R., Chung, C. E., Clarke, A. D., Coakley, J. A., Collins, W. D., Conant, W. C., Dulac, F., Heintzenberg, J., Heymsfield, A. J., Holben, B., Howell, S., Hudson, J., Jayaraman, A., Kiehl, J. T., Krishnamurti, T. N., Lubin, D., McFarquhar, G., Novakov, T., Ogren, J. A., Podgorny, I. A., Prather, K., Priestley, K., Prospero, J. M., Quinn, P. K., Rajeev, K., Rasch, P., Rupert, S., Sadourny, R., Satheesh, S. K., Shaw, G. E., Sheridan P., and Valero F. P. J.: Indian Ocean Experiment: An integrated analysis of the climate forcing and effects of the great Indo-Asian haze, *J. Geophys. Res.*, 106, 28371–28399, 2001.

Raymond, T. M. and Pandis, S. N.: Formation of cloud droplets by multicomponent organic particles, *J. Geophys. Res.*, 108, 4469, doi:10.1029/2003JD003503, 2003.

Roberts, G. C. and Nenes, A.: A continuous-flow streamwise thermal-gradient CCN chamber for atmospheric measurements, *Aerosol Sci. Tech.*, 39, 206–221, 2005.

Rose, D., Gunthe, S. S., Mikhailov, E., Frank, G. P., Dusek, U., Andreae, M. O., and Pöschl, U.: Calibration and measurement uncertainties of a continuous-flow cloud condensation nuclei counter (DMT-CCNC): CCN activation of ammonium sulfate and sodium chloride aerosol particles in theory and experiment, *Atmos. Chem. Phys.*, 8, 1153–1179, doi:10.5194/acp-8-1153-2008, 2008.

Rosenfeld, D., Lohmann, U., Raga, G.B., O'Dowd, C.D., Kulmala, M., Fuzzi, S., Reissell, A., and Andreae, M. O.: Flood or Drought: How Do Aerosols Affect Precipitation?, *Science*, 321, 1309–1313, 2008.

Seinfeld, J. H. and Pandis, S. N.: *Atmospheric chemistry and physics: From air pollution to climate change*, 2 edn., John Wiley & Sons, Inc., 1225 pp., 2006.

Wang, S. and Flagan, R.: Scanning electrical mobility spectrometer, *J. Aerosol Sci.*, 20, 1485–1488, 1989.

Young, K. C. and Warren, A. J.: A reexamination of the derivation of the equilibrium supersaturation curve for soluble particles, *J. Atmos. Sci.*, 49, 1138–1143, 1992.

Zhang, Q., Ma, X., Tie, X., Huang, M., and Zhao, C.: Vertical Distributions of Aerosols under Different Weather Conditions: Analysis of In-situ Aircraft Measurements in Beijing, China, *Atmos. Environ.*, 43, 5526–5535, 2009.

Zhang, Q., Quan, J., Tie, X., Huang, M., and Ma, X.: Impact Aerosol Particles on Cloud Formation: Aircraft Measurements in Beijing, China, *Atmos. Environ.*, 45, 665–672, 2011.

Zhang, X., Smith, K. A., Worsnop, D. R., Jimenez, J. L., Jayne, J. T., and Kolb, C. E.: A numerical characterization of particle beam collimation by an aerodynamic lens-nozzle system. Part I: An individual lens or nozzle, *Aerosol Sci. Technol.*, 36, 617–631, 2002.

Zhang, X., Smith, K. A., Worsnop, D. R., Jimenez, J. L., Jayne, J. T., Kolb, C. E., Morris, J., and Davidovits, P.: Numerical characterization of particle beam collimation: Part II: Integrated aerodynamic lens-nozzle system, *Aerosol Sci. Technol.*, 38, 619–638, 2004.

ACPD

12, 1493–1516, 2012

Impact of aerosol composition

Q. Zhang et al.

Title Page

Abstract

Introduction

Conclusions

References

Tables

Figures



Back

Close

Full Screen / Esc

Printer-friendly Version

Interactive Discussion



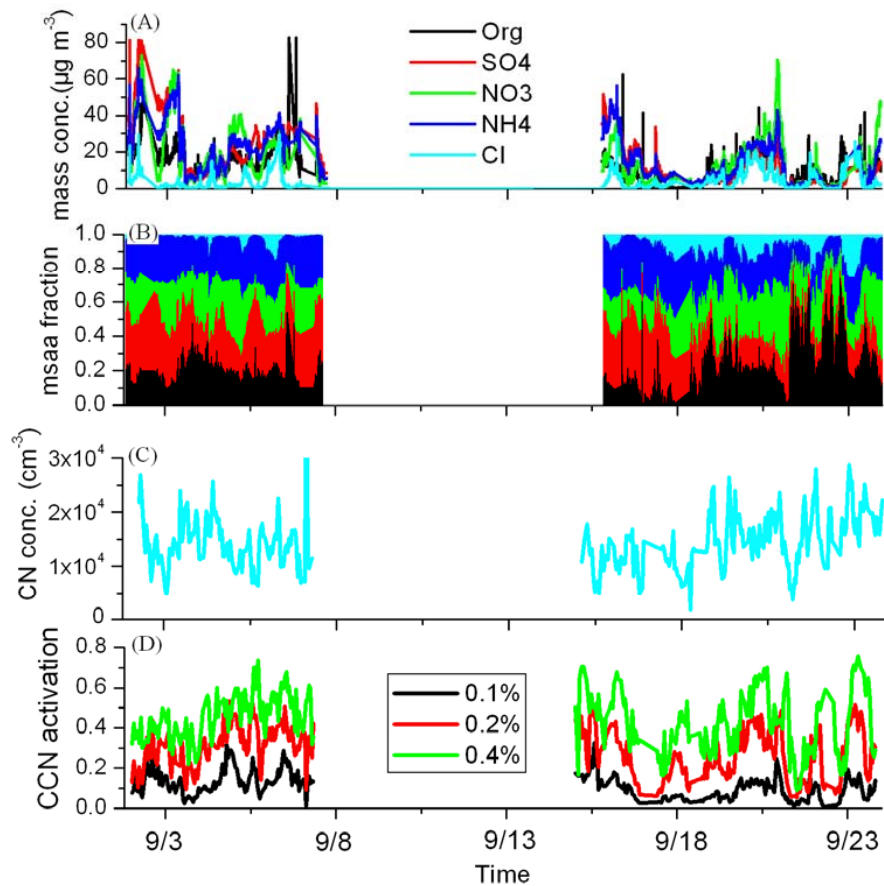


Fig. 1. The mass concentration (A), mass fraction (B) of aerosol particles observed by AMS, CN number concentration (C), and the CCN activation (CCN/CN) (D) of aerosols during the experiment.

Impact of aerosol composition

Q. Zhang et al.

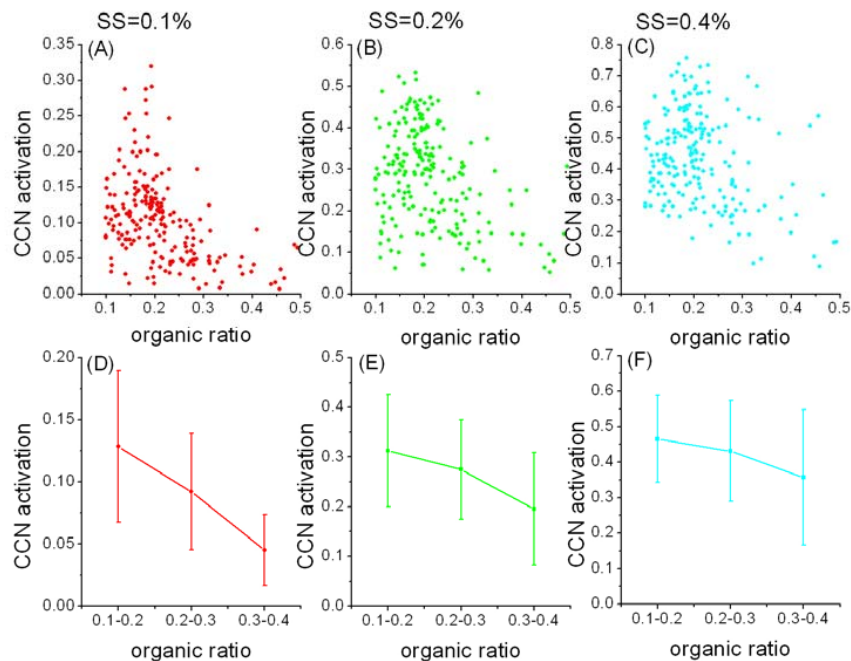


Fig. 2. the relation of CCN/CN with organics fraction under SS of 0.1%, 0.2% and 0.4%, respectively.

[Title Page](#)[Abstract](#)[Introduction](#)[Conclusions](#)[References](#)[Tables](#)[Figures](#)[◀](#)[▶](#)[◀](#)[▶](#)[Back](#)[Close](#)[Full Screen / Esc](#)[Printer-friendly Version](#)[Interactive Discussion](#)

Impact of aerosol composition

Q. Zhang et al.

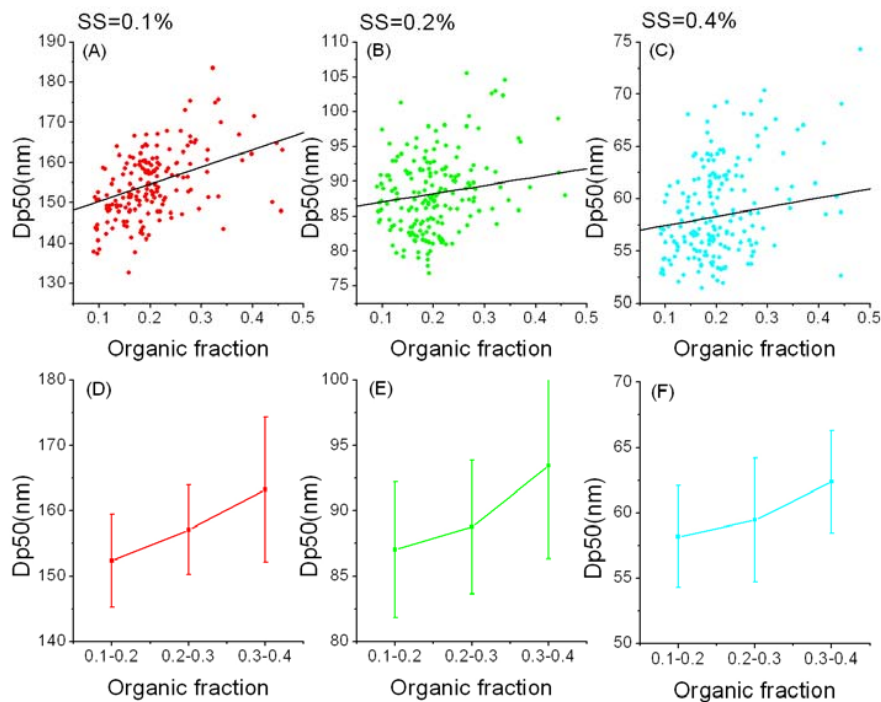


Fig. 3. The relation of Dp50 with organics fraction under SS of 0.1 %, 0.2 % and 0.4 %, respectively.

[Title Page](#)[Abstract](#)[Introduction](#)[Conclusions](#)[References](#)[Tables](#)[Figures](#)[◀](#)[▶](#)[◀](#)[▶](#)[Back](#)[Close](#)[Full Screen / Esc](#)[Printer-friendly Version](#)[Interactive Discussion](#)

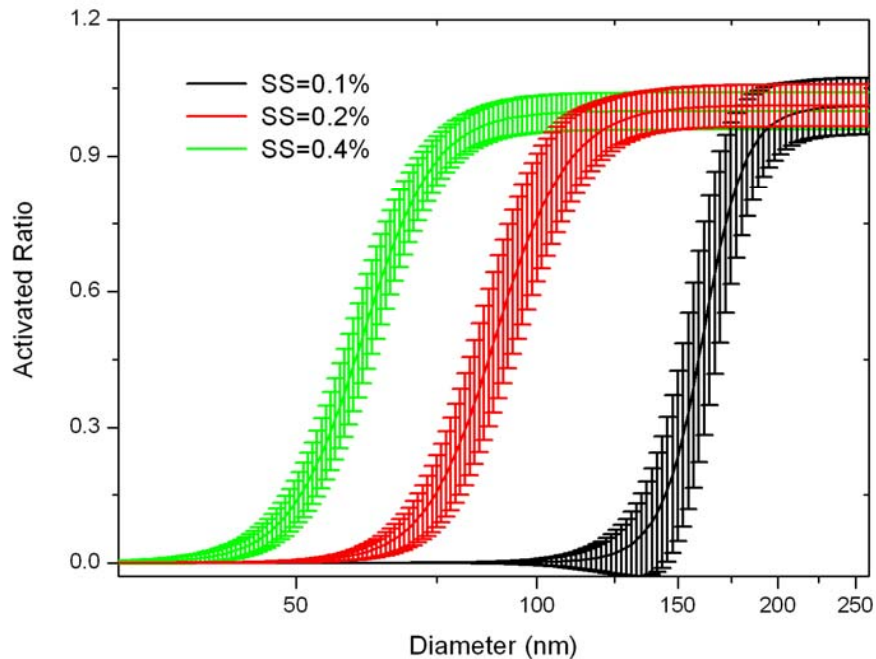


Fig. 4. The size-resolved CCN activation of aerosol particles under SS of 0.1%, 0.2% and 0.4%, respectively.

Impact of aerosol composition

Q. Zhang et al.

Title Page	
Abstract	Introduction
Conclusions	References
Tables	Figures
◀	▶
◀	▶
Back	Close
Full Screen / Esc	
Printer-friendly Version	
Interactive Discussion	



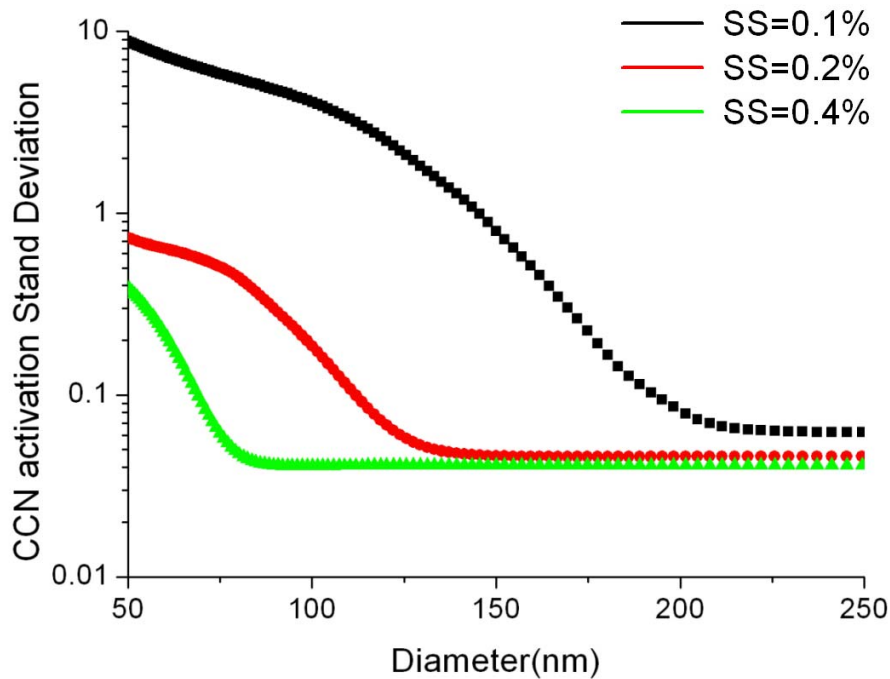


Fig. 5. the calculated stand deviation of size-resolved CCN activation under of 0.1 %, 0.2 % and 0.4 %, respectively.

Impact of aerosol composition

Q. Zhang et al.

Title Page

Abstract Introduction

Conclusions References

Tables Figures

◀ ▶

◀ ▶

Back Close

Full Screen / Esc

Printer-friendly Version

Interactive Discussion



Impact of aerosol composition

Q. Zhang et al.

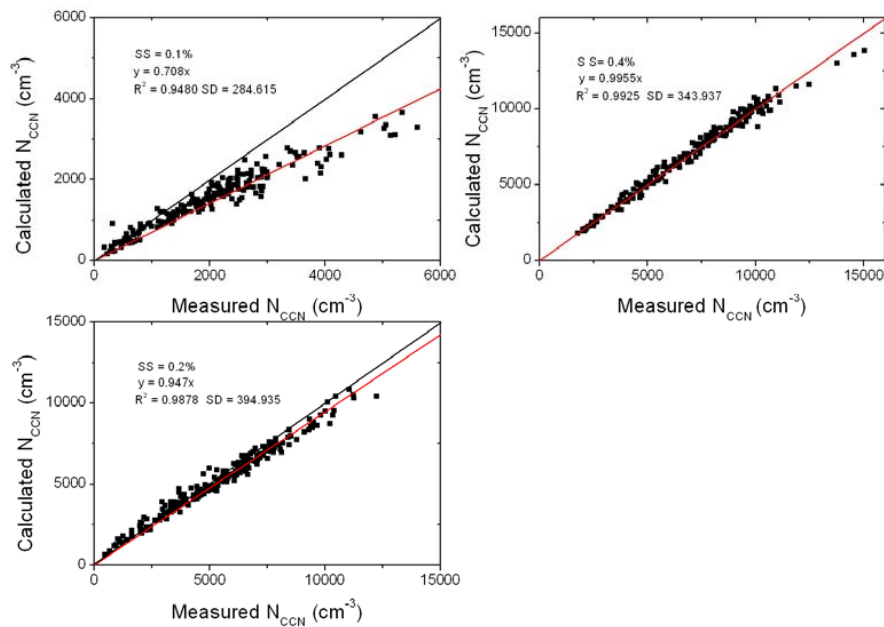


Fig. 6. Closure between measured CCN number concentration and the CCN number concentration calculated from aerosol number size distribution and size-resolved activation for the three SS.

[Title Page](#)[Abstract](#)[Introduction](#)[Conclusions](#)[References](#)[Tables](#)[Figures](#)[◀](#)[▶](#)[◀](#)[▶](#)[Back](#)[Close](#)[Full Screen / Esc](#)[Printer-friendly Version](#)[Interactive Discussion](#)

Impact of aerosol composition

Q. Zhang et al.

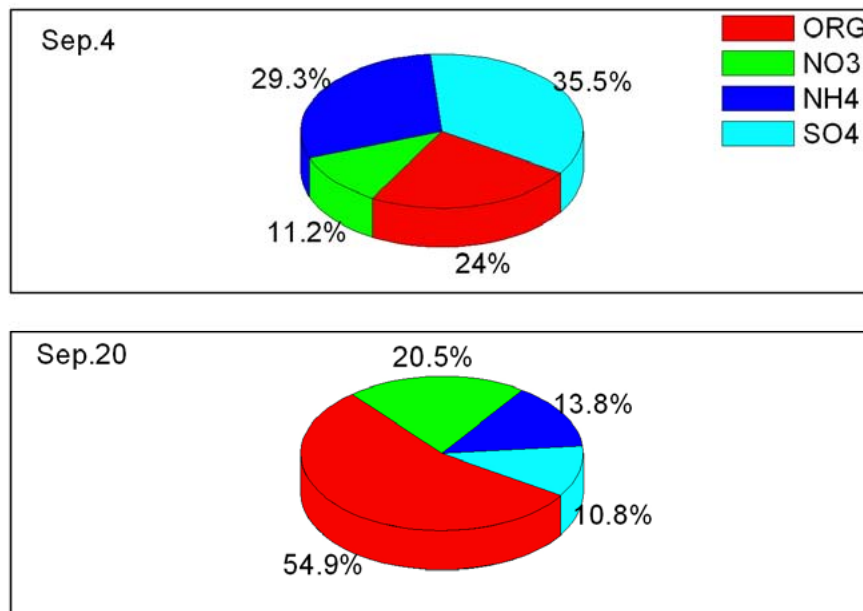


Fig. 7. the daily averaged composition of the two days with size ranging from 50 to 200 nm on 4 and 20 September 2010.

[Title Page](#)[Abstract](#)[Introduction](#)[Conclusions](#)[References](#)[Tables](#)[Figures](#)[I◀](#)[▶I](#)[◀](#)[▶](#)[Back](#)[Close](#)[Full Screen / Esc](#)[Printer-friendly Version](#)[Interactive Discussion](#)

Impact of aerosol composition

Q. Zhang et al.

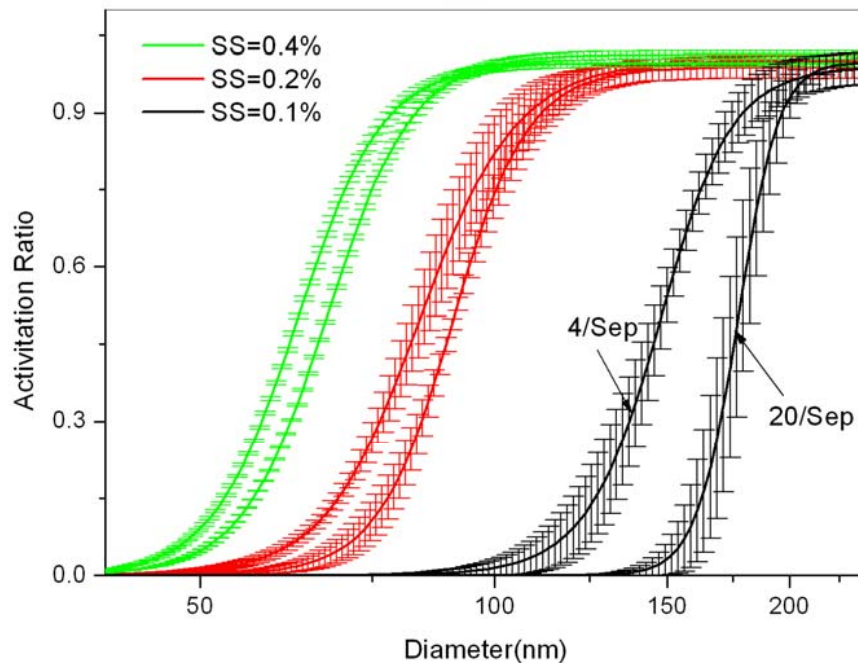


Fig. 8. The size-resolved CCN activation of aerosol particles under different SS for 4 and 20 September 2010.

[Title Page](#)[Abstract](#)[Introduction](#)[Conclusions](#)[References](#)[Tables](#)[Figures](#)[◀](#)[▶](#)[◀](#)[▶](#)[Back](#)[Close](#)[Full Screen / Esc](#)[Printer-friendly Version](#)[Interactive Discussion](#)